Supporting Material

Supporting Figures 1 - 4 and Table

Limitations of constant-force-feedback experiments

Phillip Elms[1,3], John D. Chodera[3], Carlos Bustamante[2,3,4,5], and Susan Marqusee[2,3]

[1]Biophysics Graduate Group, [2]Department of Molecular and Cell Biology, [3]California Institute for Quantitative Biosciences (QB3), [4]Department of Physics, [5]Howard Hughes Medical Institute, University of California, Berkeley, CA 94720-3220, USA

Corresponding Authors:

Susan Marqusee

576 Stanley Hall, University of California - Berkeley

Berkeley, CA 94720-3220

Email: marqusee@berkeley.edu

Carlos Bustamante

608A Stanley Hall, University of California - Berkeley

Berkeley, CA 94720-3220

carlos@alice.berkeley.edu

Effect of Force on Rate Constants

Using the order parameter, the end-to-end extension of a molecule, to define the reaction coordinate, the simplest model that describes how a constant applied force will affect the rate constant is a linear free energy relationship, such as that given by Bell [1],

$$k(F) = k_m k_0 \exp\left(\frac{F\Delta x^{\ddagger}}{k_B T}\right) \qquad (1)$$

where k_m includes the contributions of bead size, trap stiffness, and other components of the experimental system to the observed rates, k_0 is the intrinsic rate constant in the absence of force, F is the applied force, $\Delta x^{\ddagger}$ is the distance to the transition state, k_B is the Boltzmann constant, and T is the absolute temperature. This model assumes that the position of the transition state does not change as a function of force. Geometrically, this algebraic relationship can be thought of as tilting the energy landscape from a reference position (Supporting Figure 1a and Supporting Figure 2) [2]. Two examples of constant force experimental approaches are magnetic tweezers [3] and passive all-optical force clamp [4]. For these two methods, the spring constant is very close to zero ($< 10^{-3}$ pN/nm) and therefore the effective force does not change over the range of molecular extensions observed in the experiment. Magnetic tweezers are not amenable to the types of experiments addressed in this paper due to the limitations of the distance resolution.

Alternatively, in an experiment with a trap held at constant position (Supporting Figure 3), the applied force varies with the position of the bead in the trap and is well-

approximated by a harmonic potential over the extension ranges observed in the experiment, and the above relation (Supporting Equation 1) must be modified to include the effective spring constant of the system,

$$k(F) = k_m k_0 \exp\left(\frac{F\Delta x^{\ddagger} - \frac{1}{2}\kappa\Delta x^{\ddagger 2}}{k_B T}\right) \quad (2)$$

where κ is the effective spring constant of the system. This relationship can be rewritten as,

$$\ln k(F) = \ln k_m + \ln k_0 + \frac{F\Delta x^{\ddagger}}{k_B T} - \frac{\kappa\Delta x^{\ddagger 2}}{2k_B T} \quad (3)$$

In this notation, the applied force and effective spring constant of the system are positive and the distance to the transition state is positive from the folded to the unfolded state and negative for the unfolded to folded state. This relationship shows that the change in the rate constants as a function of force (i.e. the slope of ln(k) v. force which is proportional to the distance to the transition state) is independent of the effective spring constant of the system. This relationship assumes that the experiment is done over a distance range where the trap and tether behave as a Hookean spring (i.e. the effective spring constant of the system is constant) and the potential is therefore well-modeled by a simple harmonic. It is important to note that this is the appropriate relationship to consider when using the active force feedback setup because of the finite response time of the feedback.

Compared to constant force experiment with an effective spring constant of zero, a positive effective spring constant (κ) results in an increased transition state barrier height, increasing the average lifetime of each state. As depicted in Supporting Figure 1 b and c,

this increased barrier height results for both positive and negative changes in the extension of the system, that is, for both unfolding and folding events. Because the barrier heights are affected by the magnitude of the spring constant, the average lifetime of a state measured at an average force is dependent on the effective spring constant of the system. For a negative effective spring constant, the effective barrier heights are lowered and the effect is the opposite: shorter average lifetimes at the measured average force.

This effect of the spring constant on the measured rate constants has some important consequences. Supporting Figure 4 depicts the difference between the measured rate constants of a constant-force and constant-trap-position experiment with a positive effective spring constant for a symmetrical landscape (a), where distances to the transition state are equal, and for an asymmetric landscape (b), where distances to the transition state are not equal. For a symmetric landscape, the energetic contribution from the effective spring constant of the system is the same for both folding and unfolding and therefore there is an equal shift in both the folding and unfolding rate constants. While the rate constants change with the spring constant of the system, the distance to the transition state, which is proportional to the slope of the line, and the force at which the rate constants for folding and unfolding are the same (i.e. the coincident rate constant), remain unchanged. However, for an asymmetrical landscape, there is a change in the force of the coincident rate constant. Therefore, because the experiments carried out under these non-constant force conditions are not at equilibrium with respect to each other at the same average force, the equilibrium constants cannot be defined at a given

force by the ratio of the rate constants at that defined force without accounting for the contribution from the effective spring constant of the system. In spite of this, the slopes, or distance to the transition state, remain unchanged for the asymmetric landscape.

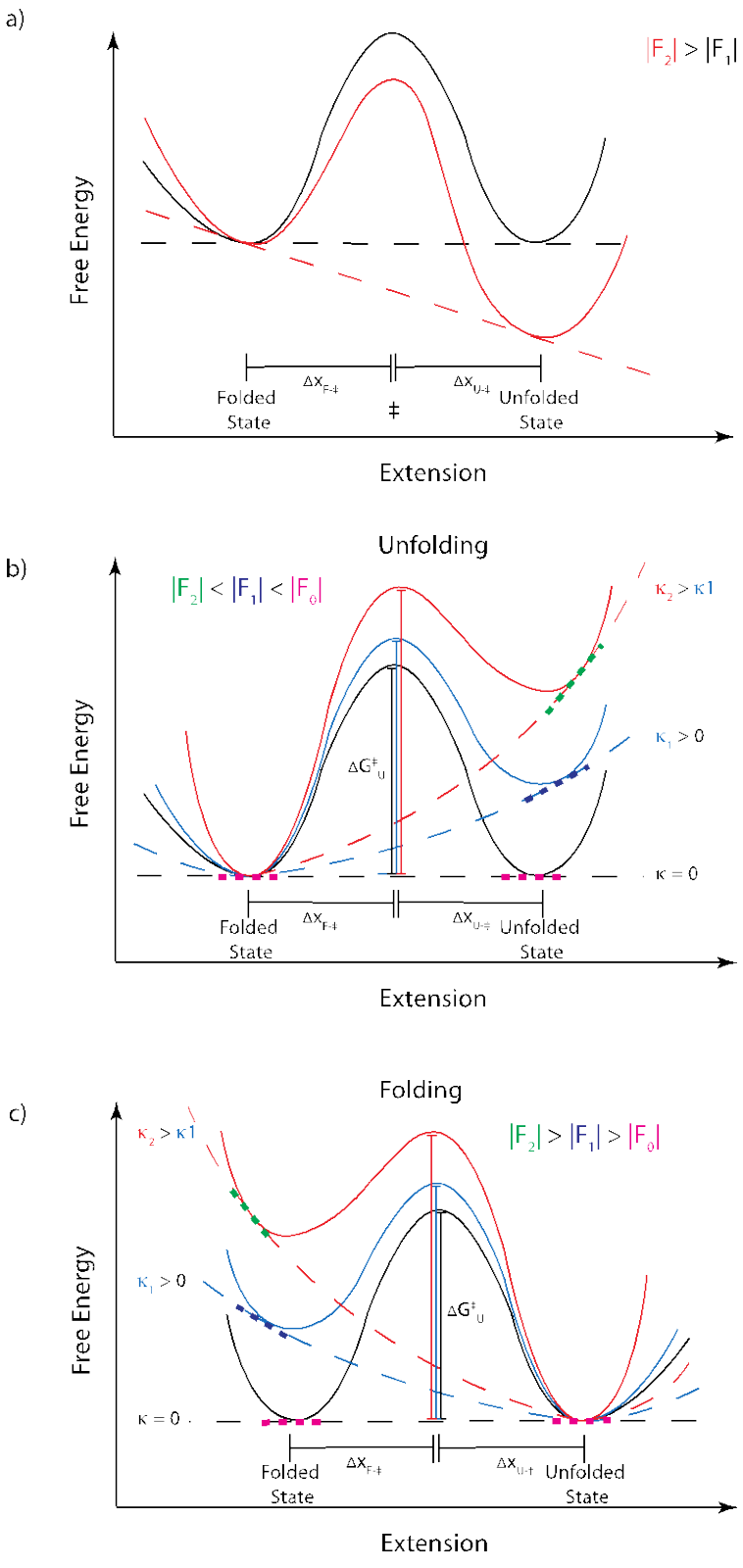

Supporting Figure 1. The effect of force on a potential energy landscape.

Supporting Figure 1. The effect of force on a potential energy landscape.

For a constant force, the difference in the energy of two states is shown (**a**) at two arbitrary forces with an effective spring constant of zero and with F_2 greater than F_1. The slope of the dotted line indicates the force on the state. The higher force changes the energy of the system such that the more extended state is the lower energy state. In **b** and **c**, the potential energy surface is shown for a positive and negative extension change (unfolding and folding, respectively) at various arbitrary spring constants. The folded state in **b** and the unfolded state in **c** are depicted at the same average force. This illustrates the change in the effective barrier heights with a change in the effective spring constants of the system compared for the same state at the same average force.

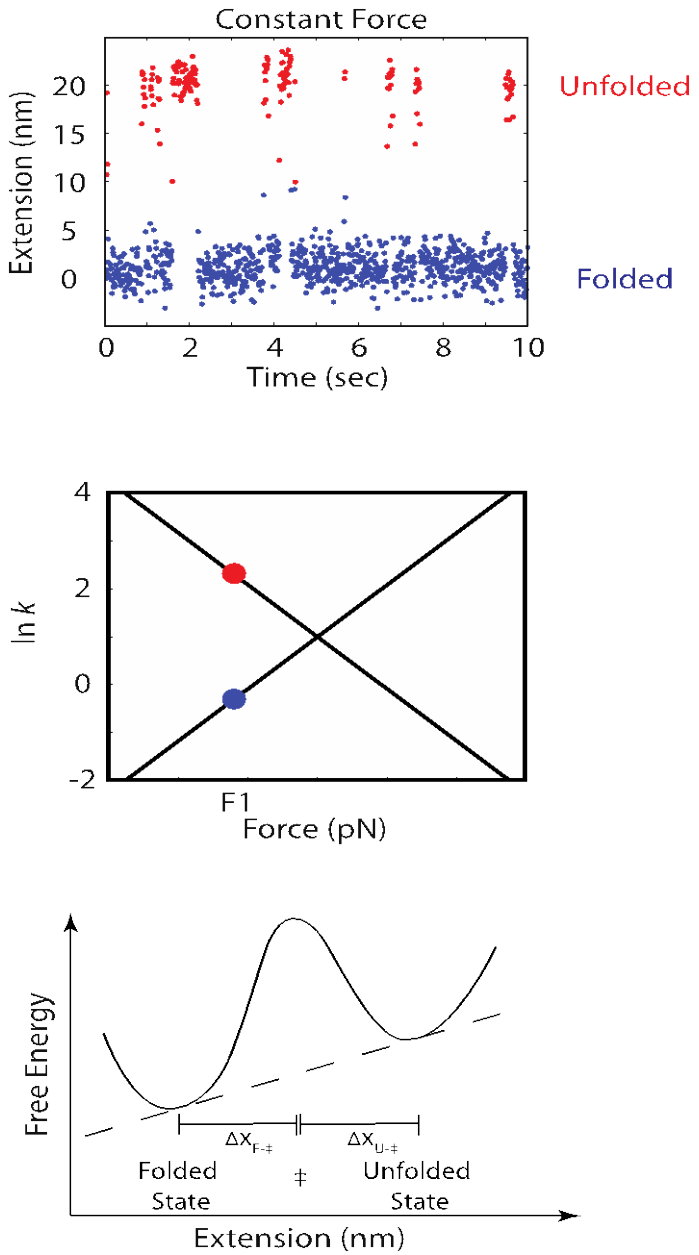

Supporting Figure 2. Illustration of constant-force experimental data and results.

This figure depicts the data from a constant-force experiment, the corresponding plot of the measured rate constants as a function of the average force, and the underlying energy landscape for the two state system at a single constant average force.

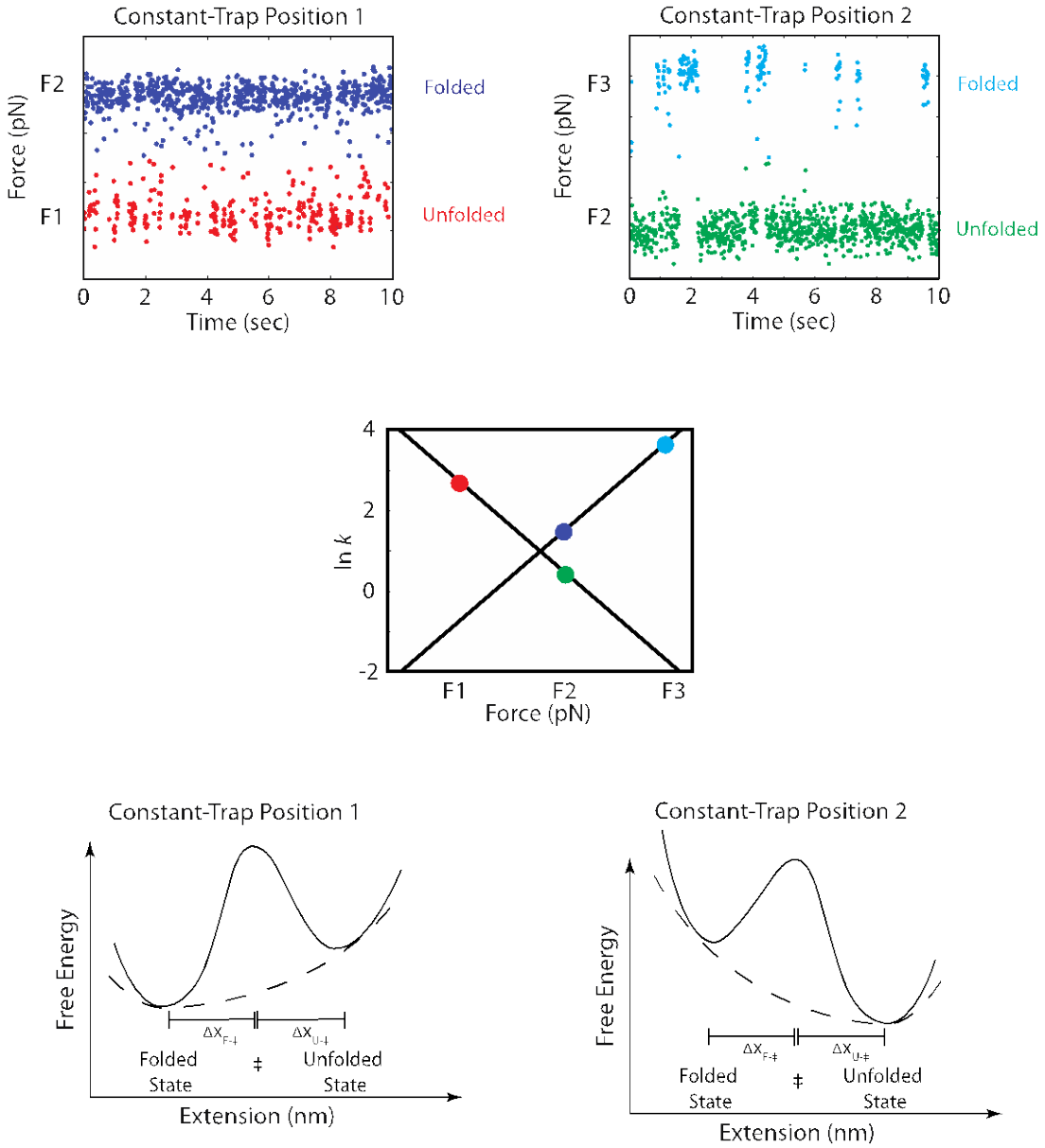

Supporting Figure 3. Illustration of constant-trap-position experimental data and results.

Supporting Figure 3. Illustration of constant-trap-position experimental data and results.

This figure depicts the data from two different constant-trap-position experiments, the corresponding plot of the measured rate constants as a function of the average force, and the underlying energy landscape of the two state system at both trap positions.

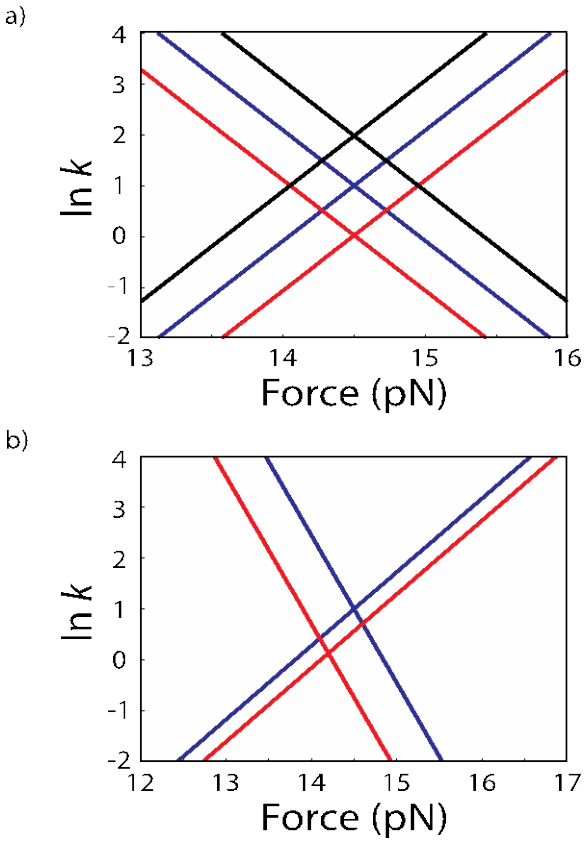

Supporting Figure 4. Comparison of the rate constants measured from a constant-force and constant-trap-position experiments.

The natural log of the rate constants as a function of force for a model symmetric system (**a**) ($\Delta x^{\ddagger}_{F\text{-}U} = \Delta x^{\ddagger}_{U\text{-}F}$) and for a model asymmetric system (**b**) ($2(\Delta x^{\ddagger}_{F\text{-}U}) = \Delta x^{\ddagger}_{U\text{-}F)}$) are shown. The rate constants as a function of force for a constant force, a positive spring constant (κ = 0.1 pN/nm), and a negative spring constant (κ = -0.1 pN/nm), are shown in blue, red, and black, respectively. Figure **b** illustrates the change in the rate constants as a function of force between a constant-force experiment (in blue) and a positive spring constant (in red) for a system with an asymmetric landscape. An important consequence is the change in the force of coincident rate constant and the change in the calculated apparent equilibrium constants as a function of force.

Supporting Table 1. Results from the linear fits of the constant-force- feedback and constant-trap-position experiments for each individual molecule.

Molecule	$\Delta x^{\ddagger}_{Unfolding}$ (nm)[1]	$\Delta x^{\ddagger}_{Folding}$ (nm)[1]	Δx_{Total}(Sum) (nm)[1]	Δx_{Total}(Measured) (nm)[2]	Ratio of $\Delta x_{Total}{}^{3}$	$\ln(k_{Coincident})$[1]
Constant-Force Feedback (Partition Method 100 Hz)						
DNA Hairpin						
Fiber 1	11.1 ± 1.2	11.9 ± 0.5	23.0 ±1.3			1.2
Fiber 2	11.8 ± 1.5	12.8 ± 0.8	24.6 ± 1.7			1.6
Fiber 3	11.1 ± 1.5	11.8 ± 0.4	22.9 ± 1.5			1.1
Fiber 4	11.3 ± 1.0	12.6 ±1.6	24.0 ± 1.9			1.3
Fiber 5	11.3 ± 1.6	11.5 ±2.8	22.8 ± 3.2			1.3
Average	11.3 ± 0.6	12.1 ± 1.1	23.5 ± 1.6	17.7 ± 0.4	1.33	1.3 ± 0.4
RNA Hairpin						
Fiber 1	12.3 ± 1.6	12.8 ± 1.8	25.1 ± 2.4			1.0
Fiber 2	12.6 ± 1.9	13.4 ± 8.4	26.0 ± 8.6			0.7
Fiber 3	14.7 ± 4.7	13.6 ± 6.1	28.3 ± 7.7			0.6
Fiber 4	11.4 ± 3.6	16.2 ± 3.5	27.6 ± 5.0			1.0
Fiber 5	11.3 ± 1.7	15.0 ± 2.9	26.3 ± 3.4			1.1
Fiber 6	11.7 ± 1.6	13.3 ± 0.8	25.0 ± 1.8			1.1
Fiber 7	11.0 ± 1.4	12.7 ± 0.9	23.7 ± 1.7			1.0
Average	12.1 ± 2.5	13.9 ± 2.6	26.0 ± 3.2	19.2 ± 0.4	1.35	0.9 ± 0.4
Protein						
Fiber 1	16.8 ± 2.1	21.8 ± 3.4	38.6 ± 4.0			1.9
Fiber 2	10.4 ± 4.3	28.3 ± 5.3	38.7 ± 6.8			2.1
Fiber 3	19.3 ± 1.3	19.8 ± 7.9	39.1 ± 8.0			2.4
Fiber 4	9.5 ± 1.9	23.4 ± 5.3	32.9 ± 5.6			2.1

Fiber 5	17.9 ± 15.6	21.5 ± 7.0	39.4 ± 17.1			1.5
Fiber 6	14.6 ± 3.1	19.7 ± 2.1	34.3 ± 3.7			1.7
Average	14.8 ± 8.1	22.4 ± 6.4	37.2 ± 5.6	18.9 ± 0.4	1.97	2.0 ± 0.6

Constant-Trap Position (Partition Method 100 Hz)

DNA Hairpin						
Fiber 1	8.3 ± 1.7	10.8 ± 2.5	19.0 ± 3.0			1.3
Fiber 2	8.7 ± 1.7	11.2 ± 0.8	19.9 ± 1.9			1.5
Fiber 3	10.4 ± 1.2	11.6 ± 1.7	21.9 ± 2.1			1.7
Fiber 4	9.5 ± 1.2	9.1 ± 6.2	18.6 ± 6.3			0.9
Fiber 5	9.5 ± 1.2	11.2 ± 0.4	20.7 ± 1.3			1.1
Fiber 6	9.1 ± 1.7	11.6 ± 1.2	20.7 ± 2.1			1.3
Fiber 7	9.5 ± 1.2	11.2 ± 1.2	20.7 ± 1.8			1.2
Average	9.3 ± 1.4	10.9 ± 1.8	20.2 ± 1.5	17.7 ± 0.4	1.14	1.3 ± 0.6
RNA Hairpin						
Fiber 1	11.2 ± 1.2	14.5 ± 2.1	25.7 ± 2.4			0.5
Fiber 2	7.9 ± 0.8	15.3 ± 2.5	23.2 ± 2.6			1.4
Fiber 3	12.4 ± 1.2	10.8 ± 0.8	23.2 ± 1.5			0.6
Fiber 4	6.6 ± 1.2	12.8 ± 0.8	19.5 ± 1.5			0.6
Fiber 5	6.2 ± 1.2	12.4 ± 0.8	18.6 ± 1.5			1.3
Average	8.9 ± 5.6	13.2 ± 3.6	22.1 ± 6.6	19.2 ± 0.4	1.15	0.9 ± 0.9
Protein						
Fiber 1	8.7 ± 4.1	15.3 ± 7.5	24.0 ± 8.5			3.0
Fiber 2	6.6 ± 1.7	16.6 ± 3.3	23.2 ± 3.7			2.2
Fiber 3	9.5 ± 3.7	12.0 ± 4.1	21.5 ± 5.6			2.3
Fiber 4	5.8 ± 1.2	19.0 ± 1.7	24.8 ± 2.1			2.3
Fiber 5	7.0 ± 0.8	16.6 ± 1.7	23.6 ± 1.9			2.2

Average	7.5 ± 3.1	15.9 ± 5.1	23.4 ± 6.0	18.9 ± 0.4	1.24	2.4 ± 0.7

Constant-Trap Position (BHMM Method 1000 Hz)

DNA Hairpin						
Fiber 1	7.8 ± 1.1	10.3 ± 2.0	18.1 ± 2.3			1.9
Fiber 2	7.4 ± 0.9	10.2 ± 0.7	17.6 ± 1.1			1.5
Fiber 3	8.2 ± 0.6	10.1 ± 1.1	18.3 ± 1.3			2.0
Fiber 4	7.5 ± 0.9	9.3 ± 4.3	16.8 ± 4.4			1.7
Fiber 5	8.3 ± 0.8	10.6 ± 0.3	18.9 ± 0.9			1.3
Fiber 6	7.7 ± 0.5	10.3 ± 0.8	18.3 ± 1.0			1.7
Fiber 7	7.8 ± 0.5	10.2 ± 1.4	18.0 ± 0.9			1.6
Average	7.8 ± 0.7	10.2 ± 0.9	18.0 ± 1.3	17.7 ± 0.4	1.02	1.7 ± 0.5
RNA Hairpin						
Fiber 1	8.7 ± 0.8	13.3 ± 0.6	22.0 ± 1.0			1.4
Fiber 2	7.4 ± 1.1	11.7 ± 1.8	19.1 ± 2.1			1.7
Fiber 3	9.2 ± 0.5	10.6 ± 0.5	19.8 ± 0.7			1.4
Fiber 4	7.3 ± 0.7	11.5 ± 0.6	18.8 ± 0.9			1.0
Fiber 5	7.0 ± 0.5	10.9 ± 0.8	17.9 ± 0.9			1.8
Average	7.9 ± 1.9	11.6 ± 2.1	19.5 ± 3.1	19.2 ± 0.4	1.02	1.5 ± 0.7
Protein						
Fiber 1	6.1 ± 1.1	12.6 ± 2.3	18.7 ± 2.5			2.6
Fiber 2	6.5 ± 1.0	12.6 ± 2.3	19.1 ± 2.5			3.4
Fiber 3	6.7 ± 1.2	14.0 ± 1.9	20.7 ± 2.2			2.6
Fiber 4	5.3 ± 0.8	16.9 ± 1.3	22.2 ± 1.0			2.9
Fiber 5	5.9 ± 0.6	16.0 ± 1.3	21.9 ± 1.4			2.7
Average	6.1 ± 1.1	14.4 ± 3.9	20.5 ± 3.2	18.9 ± 0.4	1.09	2.8 ± 0.7

[1] Average values reported with a 95% confidence interval.

[2] Distance determined from fitting a histogram of the trap position from a constant-force-feedback experiment with two Gaussian distributions and determining the difference between the two Gaussian means with a 95% confidence interval.

[3] Ratio of the calculated sum of the distances to the transition state to the experimentally measured distance between the two states.

References

1. Bell, G.I., *Models for the specific adhesion of cells to cells*, in *Science*. 1978. p. 618-27.
2. Tinoco, I. and C. Bustamante, *The effect of force on thermodynamics and kinetics of single molecule reactions*, in *Biophys Chem*. 2002. p. 513-33.
3. Neuman, K.C. and A. Nagy, *Single-molecule force spectroscopy: optical tweezers, magnetic tweezers and atomic force microscopy*, in *Nat Methods*. 2008. p. 491-505.
4. Greenleaf, W.J., et al., *Passive all-optical force clamp for high-resolution laser trapping*, in *Phys. Rev. Lett.* 2005. p. 208102.